HHS Public Access

Author manuscript

Biotechnol J. Author manuscript; available in PMC 2017 May 01.

Published in final edited form as:

Biotechnol J. 2016 May ; 11(5): 662–675. doi:10.1002/biot.201500374.

Human pluripotent stem cell culture density modulates YAP signaling

Cheston Hsiao, **Michael Lampe**, **Songkhun Nillasithanukroh**, **Wenqing Han**, **Xiaojun Lian**, and **Sean P Palecek**

Department of Chemical & Biological Engineering, University of Wisconsin - Madison, Madison, WI 53706, USA

Abstract

Human pluripotent stem cell (hPSC) density is an important factor in self-renewal and differentiation fates; however, the mechanisms through which hPSCs sense cell density and process this information in making cell fate decisions remain to be fully understood. One particular pathway that may prove important in density-dependent signaling in hPSCs is the Hippo pathway, which is regulated by cell-cell contact and mechanosensing through the cytoskeleton and has been linked to the maintenance of stem cell pluripotency. To probe regulation of Hippo pathway activity in hPSCs, we assessed whether Hippo pathway transcriptional activator YAP was differentially modulated by cell density. At higher cell densities, YAP phosphorylation and localization to the cytoplasm increased, which led to decreased YAP-mediated transcriptional activity. Furthermore, total YAP protein levels diminished at high cell density due to the phosphorylation-targeted degradation of YAP. Inducible shRNA knockdown of YAP reduced expression of YAP target genes and pluripotency genes. Finally, the density-dependent increase of neuroepithelial cell differentiation was mitigated by shRNA knockdown of YAP. Our results suggest a pivotal role of YAP in cell density-mediated fate decisions in hPSCs.

Keywords

human pluripotent stem cells; YAP; cell density; self-renewal; neural differentiation

1. INTRODUCTION

The YAP/Hippo pathway has been identified as a major regulator of mammalian organ development and disease [1, 2, 3 homeostasis and disease.] that, depending on the physiological context, coordinates signaling networks that govern cell proliferation and apoptosis, stem cell self-renewal and differentiation, and cancer progression [4–7]. The core Hippo signaling pathway is composed of a series of kinases that principally target paralogous transcriptional regulators YAP and TAZ (YAP/TAZ). During low Hippo signaling activity, active YAP/TAZ localizes in the nucleus to regulate transcription,

Correspondence: Prof. Sean P Palecek, Department of Chemical & Biological Engineering, 1415 Engineering Drive, Madison, WI 53706, USA, sppalecek@wisc.edu.

CONFLICT OF INTEREST

The authors declare no financial or commercial conflict of interest.

primarily via the TEAD family transcription factors. However, upon Hippo pathway activation, upstream components promote YAP/TAZ inactivation via cytoplasmic retention, in part by promoting their interaction with 14-3-3 proteins through phosphorylation of Ser127 on YAP and Ser89 on TAZ, though other serine residues may also influence YAP and TAZ localization [8, 9]. Moreover, phosphorylation of all 5 consensus HxRxxS motifs in YAP and TAZ targets these proteins for proteosomal degradation via E3 ubiquitin ligase recruitment [10]. YAP signaling plays an important role in early development. YAP, TAZ and TEAD proteins have been connected to embryogenesis and cell fate specification [4]. TEAD family transcription factors are among the earliest genes expressed during mammalian development [11]. Early in murine development at the blastocyst stage, the trophectoderm is distinguished by nuclear-localized YAP and *TEAD* transcription, while the inner cell mass exhibits phosphorylated and cytoplasmic-localized YAP [12, 13]. The Hippo pathway has also been shown to control the pluripotency of mammalian ESCs in which YAP is found primarily in the nucleus. However, during differentiation YAP phosphorylation increases while nuclear localization and total protein levels decrease [14]. Moreover, YAP knockdown leads to loss of pluripotency while overexpression of nuclear YAP results in increased reprogramming efficiency from fibroblasts to iPSCs. TAZ was found to play a similar role in human ESCs [15]. Additionally, knockdown of *TEAD1, 3* and *4* led to loss of mouse ESC pluripotency [14].

YAP/TAZ may directly maintain “stemness” at the transcriptional level. ChIP-seq analysis of mouse ESCs identified YAP recruitment to enhancer regions of many genes that regulate pluripotency, including *OCT3/4, SOX2, NANOG*, Polycomb Group targets, BMP signaling targets, and LIF targets [14]. Furthermore, YAP and TEAD2 activated transcription of key core pluripotency transcriptional regulators such as *OCT3/4* and *NANOG* [16].

In other mammalian cell types and cancer cell lines, high density has been demonstrated to activate components of the Hippo pathway [9] and induce YAP phosphorylation and cytoplasmic retention. While the core Hippo signaling cascade is well understood, the upstream regulatory network is still being unraveled to reveal a multitude of contributors. These upstream regulators likely include components related to apical-basal polarity proteins, such as Merlin/Expanded/Kibra and Crumbs complex, and a wide array of cellular junction proteins such as E-cadherin, α/β-catenins, angiomotin, zona occludens protein and Ajuba protein [17]. In addition, cell density may be sensed through the actin cytoskeleton via stabilization of F-actin leading to YAP/TAZ activation or disruption of F-actin leading to YAP/TAZ inactivation [18]. In human pluripotent stem cells, it is unclear whether or by what mechanism cell density regulates YAP and the maintenance of pluripotency.

Thus, determining how YAP activity modulation over the range of hPSC densities commonly employed in expansion and directed differentiation protocols affects pluripotency and differentiation will be important to controlling hPSC fates. In this study, we report that as cell density increased, YAP nuclear localization decreased concomitantly with increased phosphorylation and decreased transcriptional activity. Furthermore, inducible shRNA knockdown of YAP reduced expression of YAP pathway target genes, including regulators of pluripotency. Finally, high hPSC culture density enhanced differentiation to neuroepithelial progenitors in a YAP-dependent manner.

2. MATERIALS & METHODS

2.1 hPSC culture and neuroepithelial differentiation

H9 hESCs and 19-9-11 iPSCs were cultured on 6-well and 12-well tissue culture polystyrene (TCPS) plates coated with growth factor-reduced Matrigel (BD Biosciences) for at least 1 hour at 37°C. Cells were maintained in mTeSR1 medium (STEMCELL Technologies) or, during density experiments, E8 medium [19] which consisted of DMEM/F12 (Life Technologies), 543 mg/L sodium bicarbonate (Sigma), 64 mg/L ascorbic acid (Sigma), 10.7 mg/L transferrin (Sigma), 1 mg/L insulin (Sigma), 100 μg/L FGF2 (Waisman Clinical Biomanufacturing Facility, University of Wisconsin-Madison), 14 μg/L sodium selenite (Sigma), and 2 μg/L TGFβ1 (Peprotech). E8 medium pH was adjusted to 7.4 and osmolarity to 340 mOsm with NaCl. 5 μM ROCK inhibitor (Y-27632; Stemgent) was included in medium during singularized cell seeding.

Differentiation to neuroepithelium was performed as previously described [20]. Briefly, hPSCs were seeded onto Matrigel at seeding densities of 0.5, 1.0, 1.5 or 2.0×10^5 cells/cm^2 in E8 medium containing 10μM ROCK inhibitor and cultured overnight. The next day, differentiation was started by changing the medium to E6 medium (E8 medium lacking FGF2 and TGFβ1). Medium was changed daily thereafter.

2.2 Immunostaining and Image Analysis

Cells cultured on glass coverslips coated with Matrigel were fixed with 4% paraformaldehyde (EMS) for 15 min at room temperature. Cells were permeabilized for 1 hr at room temperature in PBS with 0.4% Triton X-100 and blocked for 1 hr at room temperature in blocking buffer (PBS with 0.4% Triton X-100 and 1% bovine serum albumin (Thermo Fisher)). Fixed cells were incubated with primary antibodies (Supp. Table 1) overnight at 4°C in blocking buffer and secondary antibodies were incubated for 1 hr at room temperature in blocking buffer. Following PBS washes, nuclei were labeled with Hoechst (Life Technologies) for 5 min according to manufacturer's instructions. Samples were then rinsed in water, dried and mounted on coverslips with ProLong Gold anti-fade reagent (Life Technologies) and imaged using a Nikon A1 Confocal Laser Microscope System (Nikon). Pearson's coefficients were calculated in ImageJ and the Just Another Colocalisation Plugin [21].

2.3 Western Blot Analysis

Western blot analysis was performed as described previously [22]. Whole cells were lysed in M-PER Mammalian Protein Extraction Reagent (Pierce) and Halt Protease and Phosphatase Inhibitor Cocktail (Pierce). Cytoplasmic and nuclear extracts were isolated using a nuclear fractionation protocol described [23]. 10% Tris-Glycine SDS-PAGE was used to separate proteins under denaturing conditions, and proteins were subsequently transferred to a PVDF membrane. The membrane was blocked with 5% BSA or Milk in TBS + 0.1% Tween-20, then labeled with primary antibody overnight at 4°C. The membrane was then washed and incubated with a secondary antibody (Supp. Table 1), conjugated with horseradish peroxidase, overnight at 4°C. Proteins were quantified with SuperSignal West Pico

Chemiluminescent Substrate (Pierce). Protein loading was normalized to β-actin, GAPDH and Histone H3 levels.

2.4 RT-PCR and Quantitative RT-PCR

PCR-based gene expression analysis was performed as described previously [22]. For RNA extraction, cells were first dissociated with Accutase (Innovative Cell Technologies). Total RNA was extracted using DNA/RNA Shield with Quick-RNA MiniPrep (Zymo Research) according to the manufacturer's instructions. cDNA was produced from 1 μg of RNA via Omniscript reverse transcriptase (Qiagen) and Oligo-dT(20) primers (Life Technologies). RT-PCR was carried out with GoTaq Green Master Mix (Promega) and then 2% agarose gel electrophoresis was performed. *TBP* was used as a control. Quantitative RT-PCR (qPCR) was carried out using TaqMan® Assays (Life Technologies) on an iCycler (Bio-Rad). Primers are listed in Supp. Tables 2 and 3.

2.5 Plasmid construction, lentiviral assembly and infection of hPSCs

The YAP inducible-knockdown vector was constructed from the shYAP1 sequence (Addgene plasmid 27368) and the Tet-pLKO-puro backbone (Addgene plasmid 21915). The 4xGTIIC-Nluc Hippo Reporter vector was constructed by direct PCR from a synthetic TEAD luciferase reporter (Addgene plasmid 34615) [24, 25], NanoLuc® genetic reporter vector (pNL1.1[*Nluc*]; Promega), and pSicoR PGK puro backbone (Addgene plasmid 11586). The helper plasmids psPAX2 and pMD2.G (Addgene plasmids 12260 and 12259) were contransfected with the vectors into HEK-293TN cells (System Biosciences) for lentivirus particle assembly. Media containing virus were collected at 48, 72, 96 and 120 hr after transfection. The supernatant was first condensed using Lenti-X™ Concentrator (Clontech) according to the manufacturer's instructions for storage at −80°C and then used for hPSC infection in the presence of 6 μg/mL polybrene (Sigma). Transduced cells were cultured on Matrigel in mTeSR1 for at least 3 days and then selected and clonally isolated based on resistance to at least 1 μg/mL puromycin in mTeSR1.

2.6 Transfection of hPSCs

A synthetic TEAD luciferase reporter (Addgene plasmid 34615) was used in transfecting hPSCs to report YAP pathway related gene transcription. The plasmid was mixed with FuGENE HD Transfection Reagent (Promega) in Opti-MEM medium (Invitrogen). After incubation, the plasmid mixture was used to resuspend 1.0×10^6 singularized cells and incubated at room temperature for 10 min. Transfected cells were cultured on Matrigel in mTeSR1 for 24–48 hr.

2.7 Luciferase Assay

The luciferase assay was performed as described previously [23]. Cells were singularized using Accutase and collected by centrifugation. The cells were resuspended to the equivalent of 100,000 cells/100 μL DMEM/F12 of which 100 μl was placed in 96-Well Solid White Polystyrene Microplates (Corning). Luciferase and Nano-Luc activity were quantified via the Bright-Glo Luciferase Assay (Promega) and Nano-Glo Luciferase Assay (Promega), respectively, according to the manufacturer's instructions. A CellTiter-Glo Luminescent Cell

Viability Assay (Promega) was used to normalize luciferase signal to total cell number. Plates were read on a GloMax®-Multi+ Detection System with Instinct® Software (Promega).

2.8 Flow Cytometry

Flow cytometry was performed as described previously [22]. Cells were singularized and then fixed in 2% paraformaldehyde for 20 min at room temperature and permeabalized in ice-cold 90% methanol for 30 min. Cells were incubated with primary antibodies overnight at 4°C in PBS plus 0.1% Triton X-100 and 0.5% BSA. A FACS Caliber flow cytometer (Beckton Dickinson) was used to collect data. Data were analyzed using FlowJo.

2.9 Statistics

Mean, standard deviation, and p-values were determined using unpaired Student's t-tests.

3. RESULTS

3.1 YAP localization switches from nuclear to cytoplasmic as cell density increases

The Hippo pathway has been shown to be involved in mediating contact inhibition during the *in vitro* culture of mammalian cell lines, including HeLa and NIH-3T3 cells [26]. We first addressed whether the Hippo pathway is responsive to cell density in hPSCs, which do not exhibit contact inhibition. We monitored YAP phosphorylation and localization since YAP has been shown to regulate Hippo-mediated transcription in pluripotent stem cells [5, 14, 16, 27]. Upon activation of Hippo signaling, YAP is phosphorylated and exported from the nucleus. Therefore, if Hippo signaling is responsive to hPSC density, one would expect decreased localization of YAP to the nucleus and elevated phosphorylated YAP in the cytoplasm as cell density increases.

In order to determine whether YAP localization was directly influenced by hPSC density, hPSCs were seeded at different densities onto Matrigel-coated TCPS plates at 0.1, 0.2 and 0.4×10^5 cells/cm^2. After 2, 3 and 4 days of expansion in E8 medium, cells were counted (Supp Fig 1), fixed and stained for YAP and phospho-YAP (Ser127). At these conditions, maintenance of stem cell markers Oct4 and Nanog were confirmed via flow cytometry (Supp Fig 2).

At 2 days post-seeding, the YAP signal was strong and primarily located in the nucleus in cells seeded at all three densities (Fig 1A). At day 3, YAP remained primarily located in the nucleus, although there was greater cell-to-cell variability in the intensity of YAP immunofluorescence and some nuclei lacked detectable YAP (Supp Fig 3), especially at higher seeding densities. This trend of decreasing nuclear YAP intensity continued through day 4 when the cell density had become nearly confluent in all cultures.

The Pearson's Coefficients relating the colocalization of YAP and nuclei revealed a shift away from nuclear-localized YAP as cell density increased via either seeding density or expansion time (Fig 1C). TAZ expression was low, but its localization also transitioned out of the nucleus as density increased (Supp Fig 4). Phosphorylated YAP was weakly detected at all seeding densities shortly after plating (Fig 1B). The positive Pearson's Coefficients for

day 2 samples seeded at low density (Fig 1D) suggest nuclear localized phospho-YAP; however, these results may be an artifact of analyzing images with very low phospho-YAP expression (Fig 1B). However, by day 4 in culture, phospho-YAP was clearly excluded from the nucleus and localized in the cytoplasm, quantitatively demonstrated by negative Person's Coefficients (Fig 1B and D). We observed statistically significant changes in YAP and phospho-YAP localization, moving to the cytoplasm as cell density increased, whether from increased seeding densities or expansion in culture.

3.2 YAP phosphorylation increases with increasing cell density

In addition to visually demonstrating a change in YAP and phospho-YAP localization from the nucleus to the cytoplasm via immunofluorescence, we probed via western blot the relative amounts of nuclear and cytoplasmic YAP from hPSCs cultured at different densities. hPSCs were seeded onto Matrigel-coated TCPS plates at 0.2×10^5 cells/cm^2 (low density) and 4.0×10^5 cells/cm^2 (high density). After 2, 3 and 4 days of culture in mTeSR medium, nuclear and cytoplasmic extracts were isolated and analyzed for YAP concentration via western blot. YAP was predominantly detected in the nuclear extracts from hPSCs seeded at low density, and in both the cytoplasmic and nuclear extracts from hPSCs seeded at high density (Fig 2A).

In addition to an increase in the amount of cytoplasmic YAP, the ratio of phosphorylated to total YAP was greater at the higher cell density (Fig 2B). hPSCs seeded at high density exhibited a higher phospho-to-total YAP ratio than hPSCs seeded at low density through 4 days of expansion (Fig 2C). Moreover, the total YAP protein levels in hPSCs seeded at high density decreased over time (Fig 2D), as expected if phosphorylated YAP was tagged for proteasomal degradation. By combining analysis of YAP localization from immunofluorescent staining with western blots of YAP and phospho-YAP in nuclear and cytoplasmic fractions, we conclude that YAP localization is responsive to cell density changes in hPSCs, transitioning from nuclear to cytoplasmic-localized as cell density increases.

3.3 YAP transcriptional activity decreases at high cell density and low actin cytoskeletal tension

Since YAP regulates the expression of genes that control hPSC proliferation, self-renewal and differentiation, we investigated whether changes in YAP localization resulting from differences in hPSC density also correlated to changes in YAP-mediated transcription activity and gene expression in hPSCs. To enable a direct and quantitative assessment of YAP transcriptional activity in hPSCs, we transduced H9 hESC and 19-9-11 iPSC lines with a YAP/TEAD-responsive promoter-reporter, 4xGTIIC-Nluc (Fig 3A). Cells were seeded at densities ranging from 0.2 to 4.0×10^5 cells/cm^2 and after 2 days were harvested for luciferase assays and cell quantification via CellTiter Glo. As expected, YAP/TEAD-mediated transcriptional activity per cell decreased as hPSC seeding density increased (Fig 3B). This inverse relationship between YAP/TEAD transcriptional activity and cell density was observed on multiple substrates in addition to Matrigel, including vitronectin and StemAdhere (Supp Fig 5), indicating that cell density-mediated inhibition of YAP/TEAD transcription was not dependent on specific cell-matrix interactions.

To ascertain whether density-dependent changes in YAP/TEAD transcriptional activity regulated YAP/TEAD gene targets in hPSCs, cells were seeded at low and high densities and after 3 days of culture in mTeSR medium, RNA was harvested and assayed for expression of YAP-regulated genes by RT-PCR. A list of YAP direct gene targets was assembled from published microarray and ChIP data in HEK293T cells [26]. Targets were then screened for expression in hESCs [28] and the most significantly downregulated and upregulated genes were selected, with preference given to genes that were shown by ChIP to exhibit TEAD and YAP binding. Finally, utilizing a Hippo pathway protein-protein interaction network [29], only the genes whose encoded proteins demonstrated the lowest probability of directly interacting with Hippo pathway protein components were selected in order to restrict our analysis to genes that are expected to be downstream of YAP and the Hippo pathway.

From this analysis, expression levels of the genes *RHOF, SCARA3, STXBP6, PCTK3, SMARCA1*, and *RRM2* were analyzed to assess YAP-mediated transcription in hPSCs. *RHOF* encodes Rif, a Rho family GTPase involved in cytoskeletal organization in filopodia [30]. *SCARA3* protects cells from oxidative stress by scavenging reactive oxygen species [31]. *STXBP6*, which encodes amysin, binds components of SNARE complexes and is thought to modulate exocytosis [32]. *PCTK3*, cyclin-dependent kinase 18, also plays a role in the secretory pathway [33]. *SMARCA1* encodes an ATPase involved in nucleosome remodeling [34] while *RRM2* encodes a subunit of ribonucleotide reductase. We observed that expression of these genes was down-regulated in hPSCs seeded at high density as compared to cells seeded at low density (Fig 3C). Pluripotency markers *POU5F1, NANOG* and *SOX2* were also expressed at a lower levels in cells seeded at high density than cells seeded at low density (Fig 3C). Taken together, YAP reporter activity and expression analysis of YAP target genes suggest that the reduction of nuclear YAP in hPSCs cultured at high densities results in a downregulation of YAP pathway target gene expression.

Thus far, our data have demonstrated that YAP transcriptional activity decreases in response to high hPSC density. In order to determine whether the mechanism by which hPSCs sense density involves the actin cytoskeleton, we modulated actin microfilament assembly and evaluated the activity from the YAP/TEAD responsive reporter. H9 hESCs and 19-9-11 iPSCs transduced with the 4xGTIIC-Nluc reporter were seeded at densities ranging from 0.2 to 4.0 $\times 10^5$ cells/cm^2 on vitronectin. The following day, cells were treated with 1 μM latrunculin A (LatA), which prevents the conversion of globular G-actin into filamentous F-actin thereby disrupting actin polymerization [35], or 2 μM Oleoyl-L-α-lysophosphatidic acid (LPA), which activates RhoA and promotes actin polymerization [36]. 24 hours later, cells were harvested for luciferase assays to quantify YAP/TEAD transcriptional activity.

Across all seeding densities, LatA decreased YAP/TEAD reporter activity and LPA increased reporter activity as compared to controls (Fig 3D). Of note, in cells seeded at 0.2 $\times 10^5$ cells/cm^2, LatA treatment decreased reporter activity to levels similar to that measured in untreated cells seeded at 4.0 $\times$ 10^5 cells/cm^2. Correspondingly, in cells seeded at 1.0 and 4.0 $\times 10^5$ cells/cm^2, LPA treatment increased reporter activity to levels similar to or exceeding that measured in untreated cells seeded at 0.2 $\times$ 10^5 cells/cm^2. These results suggest that the actin cytoskeleton is a potent regulator of YAP/TEAD transcriptional

activity in hPSCs. Furthermore, these results are consistent with the decreased YAP activity observed at high hPSC culture density resulting from decreased actin polymerization.

3.4 YAP knockdown decreases YAP pathway gene expression

Thus far, our data have demonstrated that as hPSC density increases, YAP nuclear localization, total YAP concentration, and YAP-mediated transcription decrease. In order to facilitate analysis of the role of YAP at varying hPSC densities during differentiation, we transduced H9 hESC and 19-9-11 iPSC lines with a lentiviral construct to deliver a doxycycline (dox)-inducible YAP shRNA (ishYAP) (Fig 4A). These dox-inducible shRNA cell lines achieved a 70% decrease in *YAP* expression compared to scrambled sequence shRNA controls (Fig 4B). By semi-quantification of the western blot band intensities relative to β-actin and GAPDH, YAP protein levels in the dox-induced shRNA knockdown lines were also reduced by approximately 70% compared to the no dox control (Fig 4C). YAP protein levels were unaffected by expression of a scrambled shRNA (Fig 4C).

To probe whether YAP knockdown decreases YAP-mediated transcriptional activity in hPSCs, the expression of YAP target genes and the activity from the YAP/TEAD-responsive luciferase reporter were evaluated. We seeded H9 and 19-9-11 ishYAP cells at 0.2×10^5 cells/cm^2 in mTeSR with 2 μM doxycycline and treated the cells with fresh medium containing doxycycline daily for an additional 3 days. For gene expression analysis, RNA was extracted and analyzed via RT-PCR. In order to analyze YAP transcriptional activity via the luciferase reporter, the cells were then transfected with the reporter plasmid. After allowing the cells to attach overnight, the cells were treated with doxycycline for another 24 hours before being harvested for luciferase and CellTiter Glo assays.

As expected, YAP/TEAD reporter activity in the ishYAP knockdown lines decreased to 20–50% of the activity in the no doxycycline control (Fig 4D). In addition, YAP knockdown led to a decrease in expression of YAP target genes and pluripotency genes (Fig 4E). These results indicate that inducible shRNA knockdown of YAP decreased total YAP protein and also decreased YAP-mediated transcriptional activity.

3.5 YAP knock-down affects the rate of hPSC differentiation to neuroepithelial cells

We have demonstrated that hPSC culture density can modulate YAP localization, phosphorylation and transcriptional activity. We next asked whether these density-induced changes directly influence differentiation processes. To do so, we systematically manipulated cell density and YAP expression during a defined protocol for differentiating hPSCs to pure neuroepithelial progenitors [20]. hPSCs were seeded at 0.5, 1.0, 1.5 and 2.0 $\times 10^5$/cm^2 onto Matrigel overnight and harvested for analysis through day 6 of differentiation.

To assess neural conversion, we quantified the percentage of Pax6+ cells, an early determinant of neuroectoderm fate [37]. *In vitro*, Pax6+ neural progenitor cells can differentiate into cell types found in the central nervous system such as neurons, oligodendrocytes, and astrocytes [38]. Pax6+ cells were first detected at day 3 and increased in abundance through day 6 in cells seeded at all densities (Fig 5A). However, by day 4, a

greater percentage of cells seeded at densities higher than $0.5 \times 10^5/cm^2$ expressed Pax6. This density-dependent increase in Pax6 differentiation rate continued through day 6.

We next hypothesized that YAP knockdown at lower starting densities would increase the Pax6 conversion kinetics by reducing expression of YAP target genes, similar to the observation of low YAP target gene transcription in high-density culture. Parent and ishYAP and scrambled shRNA hPSC lines were seeded at 0.5, 1.0, 1.5 and $2.0 \times 10^5/cm^2$ onto Matrigel overnight and neuroepithelial differentiation was initiated the following day with doxycycline added daily to induce shRNA expression Indeed, inducing YAP knockdown throughout the differentiation protocol enhanced the rate of hPSC conversion to Pax6+ cells (Fig 5B). The largest increases to Pax6 differentiation rates were observed after day 4 of differentiation. Neither adding doxycycline to the parental line nor inducing expression of a scrambled shRNA sequence affected the rate of Pax6 conversion (Supp Fig 6 and Fig 5B). Interestingly, YAP knockdown increased neuroepithelial conversion kinetics most markedly at low density culture conditions (0.5 and $1.0 \times 10^5/cm^2$ seeding densities) without altering the total number of cells during neuroepithelial differentiation (Supp Fig 7).

In addition, differentiation of ishYAP cells seeded at $1.0 \times 10^5/cm^2$ was allowed to continue through Day 18 with or without doxycycline. Both induced and noninduced samples continued to differentiate towards neurons, as indicated by expression of Nestin, a neuronal precursor marker, and βIII-tubulin, a neuron-specific marker (Supp Fig 8 A–D). However, cultures that underwent continued YAP knockdown contained lower fraction of Nestin-positive cells, yet an over 3-fold higher percent of βIII-tubulin positive cells, as compared to cells without YAP knockdown, which indicated augmented progression towards neurons (Supp Fig 8E–F). Moreover, the βIII-tubulin positive cells formed during continual YAP knockdown exhibited more extensive neurite projections, as illustrated in immunofluorescent images. Together, these results indicated that kinetics and extent of hPSC differentiation to neuroepithelial progenitors and neurons under adherent conditions can be affected by seeding density in a YAP-dependent manner.

4. DISCUSSION

4.1 Relationship between cell culture density and YAP signaling in undifferentiated hPSCs

Though much has been discovered regarding the role of Hippo pathway and its transcriptional activator YAP in mammalian organ size control, tissue-specific stem cells, and cancer [1], only recently has Hippo-mediated regulation of pluripotent stem cell fates been discovered [39, 40]. Our work demonstrates that YAP localization, phosphorylation and transcriptional activity are sensitive to hPSC cell densities that are typically encountered during maintenance and directed differentiation protocols, as shown schematically in Fig 6. We observed that elevated cell densities, resulting from high seeding density and expansion in culture, resulted in a transition of YAP localization out of the nucleus towards destruction in the cytoplasm. In association, we observed decreased total YAP concentrations and a higher ratio of phosphorylated YAP to total YAP in hPSCs seeded at high densities as compared to hPSCs seeded at low densities. Consequently, YAP target gene expression and YAP/TEAD reporter activity were downregulated with increasing hPSC density. In addition, we demonstrated that the rate of hPSC differentiation to Pax6+ neuroepithelial progenitors

increased with cell density and the rate of differentiation in low density cultures increased upon YAP knockdown. Finally, we demonstrated that modulating the actin cytoskeleton regulated YAP transcriptional activity. Our results point to cell density-mediated regulation of hPSC fates via YAP regulation.

Direct evidence linking the Hippo pathway and YAP activity to cell culture density in mammalian cells was revealed by Zhao et al. [9], who demonstrated that high density culture of NIH 3T3 and MCH10A cell lines induced YAP phosphorylation and increased YAP localization to the cytoplasm. However, it is not yet clear whether mammalian cell density is sensed primarily through cell-cell contact machinery or through mechanosensing via actin cytoskeletal tension and integrity. Adherens junction components E-cadherin, β-catenin and α-catenin, all of which are important in maintaining hPSC pluripotency and self-renewal [41–43], have been identified as regulators of YAP [44–46]. E-cadherin homophilic binding decreased proliferation while disruption of cell-cell contact in murine epithelial cells resulted in YAP/TAZ nuclear localization [47]. However, more work remains in hPSCs to determine whether increasing amounts of E-cadherin and catenins via stabilized adherens junctions significantly modulate YAP localization and activity.

High apical levels of filamentous actin (F-actin) and stress fibers due, for example, to cell spreading on stiff surfaces or at low cell density, inhibits Hippo signaling and maintains nuclear localization of YAP/TAZ [48, 49]. At lower cytoskeletal tension in a more mechanically compliant cell microenvironment (e.g. softer substrates or cell crowding), cells contain less F-actin and less nuclear YAP/TAZ [24]. The regulation of YAP/TAZ by cellular tension is communicated through the actin cytoskeleton, likely via angiomotin proteins [18, 50]. Our work establishes that hPSCs can respond to cell culture density through YAP, and suggests that the mechanism by which these cells sense density involves the actin cytoskeleton.

4.2 Role of YAP in mediating density-dependent hPSC differentiation

Over 4 days of hPSC expansion, YAP levels and transcriptional activity can decrease dramatically. We probed whether this YAP downregulation could modulate downstream differentiation fates. Indeed, the rate of neuroepithelial differentiation was enhanced by increasing seeding density, thereby decreasing YAP activity, or by decreasing YAP levels via inducible shRNA expression. Many studies have implicated YAP as a regulator of neural progenitors and development. YAP and TAZ are expressed throughout the developing nervous system [51], and YAP and TEAD2 are highly expressed in neural stem cells [4]. In fact, YAP and TEAD regulate *PAX3* transcription and maintain neural progenitors (Sox2+) and neural crest progenitors (Pax3+) in an undifferentiated state [52, 53]. Similarly, loss of function in upstream effectors of YAP/TAZ, such as NF2, FAT4 and DCHS1, during neural development led to increased YAP/TAZ protein levels and nuclear localization, which resulted in an enhancement of neuroepithelial progenitor self-renewal, but reduced differentiation into neurons [54, 55]. The imbalanced self-renewal of progenitor cells impaired the developmental progression and led to malformation phenotypes such as neural tube defects and hippocampus size reduction, which could be rescued by YAP inhibition. While YAP and TEAD gain of function experiments led to enhanced expansion of neural

progenitor cells via cell cycle progression and inhibition of differentiation, loss of function led to premature neuronal differentiation [56]. Thus, in our study, decreased YAP from either high density culture or shRNA knockdown may have tipped the balance towards further neuroepithelial differentiation.

Indeed, YAP knockdown increased differentiation kinetics of hPSCs to Pax6+ cells at low cell densities (e.g. 0.5 and 1.0 × 10^5/cm^2), elevating the kinetics to those observed in hPSCs seeded at higher densities. The accelerated differentiation due to YAP knockdown became less pronounced at the higher seeding densities, such as 2.0 × 10^5/cm^2. This may indicate a limit at which decreasing YAP activity beyond does not further enhance neural differentiation. In addition, other mechanisms important to neuroepithelial differentiation, such as secreted autocrine or paracrine factors, ECM deposition and cell-cell interactions [57], may increase in a density-dependent manner and overshadow the effects of YAP knockdown at high cell densities.

It has been established that cell density affects expansion and neural differentiation in stem cells but the mechanism remains poorly understood. Tropepe et al. observed that primary tissue-derived neural stem cells underwent greater than proportional proliferation from EGF at high plating density as compared to low plating density [58]. In fact, among different neuronal differentiation protocols in murine embryonic stem cells, the starting cell density was shown to have prominent effects on the yield and purity of the derived neuronal cells [59]. In the publication first establishing a protocol for the robust generation of hPSC-derived neuroepithelial cells under adherent conditions using dual inhibition of SMAD signaling, Chambers et al. indicated that higher initial hPSC plating density favored higher ratios of neural (PAX6+) to neural-crest (HNK1+, p75+) cells [60]. Lippmann et al. demonstrated that while seeding density did not affect final percentage of hPSC-derived Pax6-expressing cells, lower seeding densities (<0.5 × 10^5 cells/cm^2) led to decreased cell outgrowth and diminished rosette formation [20]. Here, we demonstrated that seeding density affects kinetics of neuroepithelial conversion in hPSCs. Thus, our data are consistent with previous studies that suggested higher seeding densities were optimal for the *in vitro* transition of hPSCs to definitive neuroepithelium under adherent conditions.

While cell density is known to be a factor in stem cell fate decisions, other microenvironmental effectors of YAP and the Hippo pathway, such as substrate stiffness, have also been shown to affect stem cell fates. In mesenchymal stem cells, decreased substrate stiffness has been demonstrated to promote expression of neural markers, as opposed to higher stiffnesses being myogenic and osteogenic [61]. Likewise in neural progenitor and stem cells, softer substrates have been shown to promote neuronal differentiation while higher stiffness substrates promoted astrocyte and glial differentiation [62, 63]. The rate of neural stem cell proliferation and neuronal maturation has been shown to increase with decreasing substrate stiffness [64, 65]. However, only very recently has the Hippo pathway been implicated in linking substrate stiffness and cytoskeletal tension to neural differentiation in hPSCs. Sun et al. used PDMS micropost arrays to provide hPSCs with a bulk elastic modulus 3 to 4 orders of magnitude lower than glass coverslips [66]. Upon neuroepithelial induction via dual Smad inhibition, hPSCs differentiated on the soft PDMS substrates exhibited a significantly greater purity of Pax6+ neuroepithelial cells than

hPSCs differentiated on rigid glass substrates. Upon further neural induction, the purity and yield of functional motor neurons was also improved on PDMS as compared to glass. YAP and TAZ were more extensively phosphorylated and exhibited less nuclear localization in hPSCs cultured on PDMS as compared to glass. Of note, the seeding densities implemented by Sun et al. were equivalent to the lowest seeding densities we tested. Thus, YAP modulation by substrate stiffness and cell density may be complementary in directing hPSC fates. Similarly, Musah et al. observed that hESCs cultured on compliant synthetic hydrogels with an elastic modulus of approximately 0.7 kPa could differentiate to neurons, even when cultured in the self-renewal medium mTeSR, though the neuronal differentiation rate was increased upon removal of pluripotency maintaining growth factors such as bFGF and TGF-β [67]. These studies demonstrate the influence of substrate stiffness on the actin cytoskeleton, YAP activity and neuronal differentiation. Our work establishes that YAP activity is also sensitive to hPSC culture density and suggests that density-dependent effects on YAP are mediated by the actin cytoskeleton and can affect differentiation fates, such as the rate of neuroepithelial differentiation.

Supplementary Material

Refer to Web version on PubMed Central for supplementary material.

Acknowledgments

We thank the WiCell Research Institute and BIONAnocomposite Tissue Engineering Scaffolds theme in the Wisconsin Institutes for Discovery for providing cell lines, reagents and equipment. The PAX6 monoclonal antibody developed by Atsushi Kawaka was obtained from the Developmental Studies Hybridoma Bank, created by the NICHD of the NIH and maintained at The University of Iowa, Department of Biology, Iowa City, IA 52242. This work was supported by National Institutes of Health Grant R01EB007534.

Abbreviations

dox	doxycycline
hPSC	human pluripotent stem cell
LatA	latrunculin A
LPA	lysophosphatidic acid
TCPS	tissue culture polystyrene

REFERENCES

1. Barry ER, Camargo FD. The Hippo superhighway: signaling crossroads converging on the Hippo/Yap pathway in stem cells and development. Curr. Opin. Cell Biol. 2013:1–7.
2. Dong J, Feldmann G, Huang J, Wu S, et al. Elucidation of a universal size-control mechanism in Drosophila and mammals. Cell. 2007; 130:1120–1133. [PubMed: 17889654]
3. Varelas X. The Hippo pathway effectors TAZ and YAP in development, homeostasis and disease. Development. 2014; 141:1614–1626. [PubMed: 24715453]
4. Mo J-S, Park HW, Guan KL. The Hippo signaling pathway in stem cell biology and cancer. EMBO Rep. 2014; 15:642–656. [PubMed: 24825474]
5. Ramos A, Camargo FD. The Hippo signaling pathway and stem cell biology. Trends Cell Biol. 2012; 22:339–346. [PubMed: 22658639]

6. Tremblay AM, Camargo FD. Hippo signaling in mammalian stem cells. Semin. Cell Dev. Biol. 2012; 23:818–826. [PubMed: 23034192]
7. Zhao B, Li L, Lei Q, Guan KL. The Hippo-YAP pathway in organ size control and tumorigenesis: an updated version. Genes Dev. 2010; 24:862–874. [PubMed: 20439427]
8. Lei QY, Zhang H, Zhao B, Zha ZY, et al. TAZ promotes cell proliferation and epithelial-mesenchymal transition and is inhibited by the hippo pathway. Mol. Cell. Biol. 2008; 28:2426–2436. [PubMed: 18227151]
9. Zhao B, Wei X, Li W, Udan RS, et al. Inactivation of YAP oncoprotein by the Hippo pathway is involved in cell contact inhibition and tissue growth control. Genes Dev. 2007; 21:2747–2761. [PubMed: 17974916]
10. Liu CY, Zha ZY, Zhou X, Zhang H, et al. The hippo tumor pathway promotes TAZ degradation by phosphorylating a phosphodegron and recruiting the SCF{beta}-TrCP E3 ligase. J. Biol. Chem. 2010; 285:37159–37169. [PubMed: 20858893]
11. Yagi R, Kohn MJ, Karavanova I, Kaneko KJ, et al. Transcription factor TEAD4 specifies the trophectoderm lineage at the beginning of mammalian development. Development. 2007; 134:3827–3836. [PubMed: 17913785]
12. Nishioka N, Inoue KI, Adachi K, Kiyonari H, et al. The Hippo signaling pathway components Lats and Yap pattern Tead4 activity to distinguish mouse trophectoderm from inner cell mass. Dev. Cell. 2009; 16:398–410. [PubMed: 19289085]
13. Slager HG, Good MJ, Schaart G, Groenewoud JS, Mummery CL. Organization of non-muscle myosin during early murine embryonic differentiation. Differentiation. 1992; 50:47–56. [PubMed: 1639226]
14. Lian I, Kim J, Okazawa H, Zhao J, et al. The role of YAP transcription coactivator in regulating stem cell self-renewal and differentiation. Genes Dev. 2010; 24:1106–1118. [PubMed: 20516196]
15. Varelas X, Sakuma R, Samavarchi-Tehrani P, Peerani R, et al. TAZ controls Smad nucleocytoplasmic shuttling and regulates human embryonic stem-cell self-renewal. Nat. Cell Biol. 2008; 10:837–848. [PubMed: 18568018]
16. Tamm C, Böwer N, Annerén C. Regulation of mouse embryonic stem cell self-renewal by a Yes-YAP-TEAD2 signaling pathway downstream of LIF. J. Cell Sci. 2011; 124:1136–1144. [PubMed: 21385842]
17. Mo JS, Park HW, Guan KL. The Hippo signaling pathway in stem cell biology and cancer. EMBO Rep. 2014; 15:642–656. [PubMed: 24825474]
18. Yu F-X, Guan KL. The Hippo pathway: regulators and regulations. Genes Dev. 2013; 27:355–371. [PubMed: 23431053]
19. Chen G, Gulbranson DR, Hou Z, Bolin JM, et al. Chemically defined conditions for human iPSC derivation and culture. Nat. Methods. 2011; 8:424–429. [PubMed: 21478862]
20. Lippmann ES, Estevez-Silva MC, Ashton RS. Defined human pluripotent stem cell culture enables highly efficient neuroepithelium derivation without small molecule inhibitors. Stem Cells. 2014; 32:1032–1042. [PubMed: 24357014]
21. Bolte S, Cordelières FP. A guided tour into subcellular colocalization analysis in light microscopy. J. Microsc. 2006; 224:213–232. [PubMed: 17210054]
22. Hsiao C, Tomai M, Glynn J, Palecek SP. Effects of 3D microwell culture on initial fate specification in human embryonic stem cells. AICHE J. 2014; 60:1225–1235. [PubMed: 25505348]
23. Azarin SM, Lian X, Larson EA, Popelka HM, et al. Modulation of Wnt/beta-catenin signaling in human embryonic stem cells using a 3-D microwell array. Biomaterials. 2012; 33:2041–2049. [PubMed: 22177620]
24. Dupont S, Morsut L, Aragona M, Enzo E, et al. Role of YAP/TAZ in mechanotransduction. Nature. 2011; 474:179–183. [PubMed: 21654799]
25. Larkin SB, Farrance IK, Ordahl CP. Flanking sequences modulate the cell specificity of M-CAT elements. Mol. Cell. Biol. 1996; 16:3742–3755. [PubMed: 8668191]
26. Zhao B, Ye X, Yu J, Li L, et al. TEAD mediates YAP-dependent gene induction and growth control. Genes Dev. 2008; 22:1962–1971. [PubMed: 18579750]

27. Alarcón C, Zaromytidou A-I, Xi Q, Gao S, et al. Nuclear CDKs drive Smad transcriptional activation and turnover in BMP and TGF-beta pathways. Cell. 2009; 139:757–769. [PubMed: 19914168]
28. Assou S, Le Carrour T, Tondeur S, Ström S, et al. A meta-analysis of human embryonic stem cells transcriptome integrated into a web-based expression atlas. Stem Cells. 2007; 25:961–973. [PubMed: 17204602]
29. Wang W, Li X, Huang J, Feng L, et al. Defining the protein-protein interaction network of the human hippo pathway. Mol. Cell. Proteomics. 2014; 13:119–131. [PubMed: 24126142]
30. Pellegrin S, Mellor H. The Rho family GTPase Rif induces filopodia through mDia2. Curr. Biol. 2005; 15:129–133. [PubMed: 15668168]
31. Han HJ, Tokino T, Nakamura Y. CSR, a scavenger receptor-like protein with a protective role against cellular damage causedby UV irradiation and oxidative stress. Hum. Mol. Genet. 1998; 7:1039–1046. [PubMed: 9580669]
32. Scales SJ, Hesser BA, Masuda ES, Scheller RH. Amisyn, a novel syntaxin-binding protein that may regulate SNARE complex assembly. J. Biol. Chem. 2002; 277:28271–28279. [PubMed: 12145319]
33. Palmer KJ, Konkel JE, Stephens DJ. PCTAIRE protein kinases interact directly with the COPII complex and modulate secretory cargo transport. J. Cell Sci. 2005; 118:3839–3847. [PubMed: 16091426]
34. Eckey M, Kuphal S, Straub T, Rummele P, et al. Nucleosome remodeler SNF2L suppresses cell proliferation and migration and attenuates Wnt signaling. Mol. Cell. Biol. 2012; 32:2359–2371. [PubMed: 22508985]
35. Yarmola EG, Somasundaram T, Boring TA, Spector I, Bubb MR. Actin-latrunculin A structure and function. Differential modulation of actin-binding protein function by latrunculin A. J. Biol. Chem. 2000; 275:28120–28127. [PubMed: 10859320]
36. Moolenaar WH. Lysophosphatidic Acid, a Multifunctional Phospholipid Messenger. J. Biol. Chem. 1995; 270:12949–12952. [PubMed: 7768880]
37. Zhang X, Huang CT, Chen J, Pankratz MT, et al. Pax6 is a human neuroectoderm cell fate determinant. Cell Stem Cell. 2010; 7:90–100. [PubMed: 20621053]
38. Reubinoff BE, Itsykson P, Turetsky T, Pera MF, et al. Neural progenitors from human embryonic stem cells. Nat. Biotech. 2001:19.
39. Aylon Y, Sarver A, Tovy A, Ainbinder E, Oren M. Lats2 is critical for the pluripotency and proper differentiation of stem cells. Cell Death Differ. 2014; 21:624–633. [PubMed: 24413153]
40. Mullen AC. Hippo tips the TGF-β scale in favor of pluripotency. Cell Stem Cell. 2014; 14:6–8. [PubMed: 24388171]
41. Nagaoka M, Koshimizu U, Yuasa S, Hattori F, et al. E-cadherin-coated plates maintain pluripotent ES cells without colony formation. PloS ONE. 2006; 1:e15. [PubMed: 17183641]
42. Redmer T, Diecke S, Grigoryan T, Quiroga-Negreira A, et al. E-cadherin is crucial for embryonic stem cell pluripotency and can replace OCT4 during somatic cell reprogramming. EMBO Rep. 2011; 12:720–726. [PubMed: 21617704]
43. Soncin F, Ward CM. The Function of E-Cadherin in Stem Cell Pluripotency and Self-Renewal. Genes. 2011; 2:229–259. [PubMed: 24710147]
44. Kim NG, Koh E, Chen X, Gumbiner BM. E-cadherin mediates contact inhibition of proliferation through Hippo signaling-pathway components. Proc. Natl. Acad. Sci. USA. 2011; 108:11930–11935. [PubMed: 21730131]
45. Schlegelmilch K, Mohseni M, Kirak O, Pruszak J, et al. Yap1 acts downstream of α-catenin to control epidermal proliferation. Cell. 2011; 144:782–795. [PubMed: 21376238]
46. Silvis MR, Kreger BT, Lien WH, Klezovitch O, et al. α-catenin is a tumor suppressor that controls cell accumulation by regulating the localization and activity of the transcriptional coactivator Yap1. Sci. Signal. 2011; 4:ra33. [PubMed: 21610251]
47. Varelas X, Samavarchi-Tehrani P, Narimatsu M, Weiss A, et al. The Crumbs complex couples cell density sensing to Hippo-dependent control of the TGF-β-SMAD pathway. Dev. Cell. 2010; 19:831–844. [PubMed: 21145499]

48. Fernández BG, Gaspar P, Brás-Pereira C, Jezowska B, et al. Actin-Capping Protein and the Hippo pathway regulate F-actin and tissue growth in Drosophila. Development. 2011; 138:2337–2346. [PubMed: 21525075]
49. Sansores-Garcia L, Bossuyt W, Wada KI, Yonemura S, et al. Modulating F-actin organization induces organ growth by affecting the Hippo pathway. EMBO J. 2011; 30:2325–2335. [PubMed: 21556047]
50. Mana-Capelli S, Paramasivam M, Dutta S, McCollum D. Angiomotins link F-actin architecture to Hippo pathway signaling. Mol. Biol. Cell. 2014:1–29.
51. Nejigane S, Haramoto Y, Okuno M, Takahashi S, Asashima M. The transcriptional coactivators Yap and TAZ are expressed during early Xenopus development. Int. J. Dev. Biol. 2011; 55:121–126. [PubMed: 20979024]
52. Gee ST, Milgram SL, Kramer KL, Conlon FL, Moody Sa. Yes-associated protein 65 (YAP) expands neural progenitors and regulates Pax3 expression in the neural plate border zone. PloS ONE. 2011; 6:e20309. [PubMed: 21687713]
53. Milewski RC, Chi NC, Li J, Brown C, et al. Identification of minimal enhancer elements sufficient for Pax3 expression in neural crest and implication of Tead2 as a regulator of Pax3. Development. 2004; 131:829–837. [PubMed: 14736747]
54. Cappello S, Gray MJ, Badouel C, Lange S, et al. Mutations in genes encoding the cadherin receptor-ligand pair DCHS1 and FAT4 disrupt cerebral cortical development. Nat. Genet. 2013; 45:1300–1308. [PubMed: 24056717]
55. Lavado A, He Y, Paré J, Neale G, et al. Tumor suppressor Nf2 limits expansion of the neural progenitor pool by inhibiting Yap/Taz transcriptional coactivators. Development. 2013; 140:3323–3334. [PubMed: 23863479]
56. Cao X, Pfaff SL, Gage FH. YAP regulates neural progenitor cell number via the TEA domain transcription factor. Genes Dev. 2008; 22:3320–3334. [PubMed: 19015275]
57. Solozobova V, Wyvekens N, Pruszak J. Lessons from the embryonic neural stem cell niche for neural lineage differentiation of pluripotent stem cells. Stem Cell Rev. 2012; 8:813–829. [PubMed: 22628111]
58. Tropepe V, Sibilia M, Ciruna BG, Rossant J, et al. Distinct neural stem cells proliferate in response to EGF and FGF in the developing mouse telencephalon. Dev. Biol. 1999; 208:166–188. [PubMed: 10075850]
59. Lorincz MT. Optimized neuronal differentiation of murine embryonic stem cells: role of cell density. Methods Mol. Biol. 2006; 330:55–69. [PubMed: 16846016]
60. Chambers SM, Fasano CA, Papapetrou EP, Tomishima M, et al. Highly efficient neural conversion of human ES and iPS cells by dual inhibition of SMAD signaling. Nat. Biotechnol. 2009; 27:275–280. [PubMed: 19252484]
61. Engler AJ, Sen S, Sweeney HL, Discher DE. Matrix elasticity directs stem cell lineage specification. Cell. 2006; 126:677–689. [PubMed: 16923388]
62. Saha K, Keung AJ, Irwin EF, Li Y, et al. Substrate modulus directs neural stem cell behavior. Biophys. J. 2008; 95:4426–4438. [PubMed: 18658232]
63. Seidlits SK, Khaing ZZ, Petersen RR, Nickels JD, et al. The effects of hyaluronic acid hydrogels with tunable mechanical properties on neural progenitor cell differentiation. Biomaterials. 2010; 31:3930–3940. [PubMed: 20171731]
64. Banerjee A, Arha M, Choudhary S, Ashton RS, et al. The influence of hydrogel modulus on the proliferation and differentiation of encapsulated neural stem cells. Biomaterials. 2009; 30:4695–4699. [PubMed: 19539367]
65. Teixeira AI, Ilkhanizadeh S, Wigenius Ja, Duckworth JK, et al. The promotion of neuronal maturation on soft substrates. Biomaterials. 2009; 30:4567–4572. [PubMed: 19500834]
66. Sun Y, Yong KM, Villa-Diaz LG, Zhang X, et al. Hippo/YAP-mediated rigidity-dependent motor neuron differentiation of human pluripotent stem cells. Nat. Mater. 2014; 13:599–604. [PubMed: 24728461]
67. Musah S, Wrighton PJ, Zaltsman Y, Zhong X, et al. Substratum-induced differentiation of human pluripotent stem cells reveals the coactivator YAP is a potent regulator of neuronal specification. Proc. Natl. Acad. Sci. USA. 2014:111. [PubMed: 24324143]

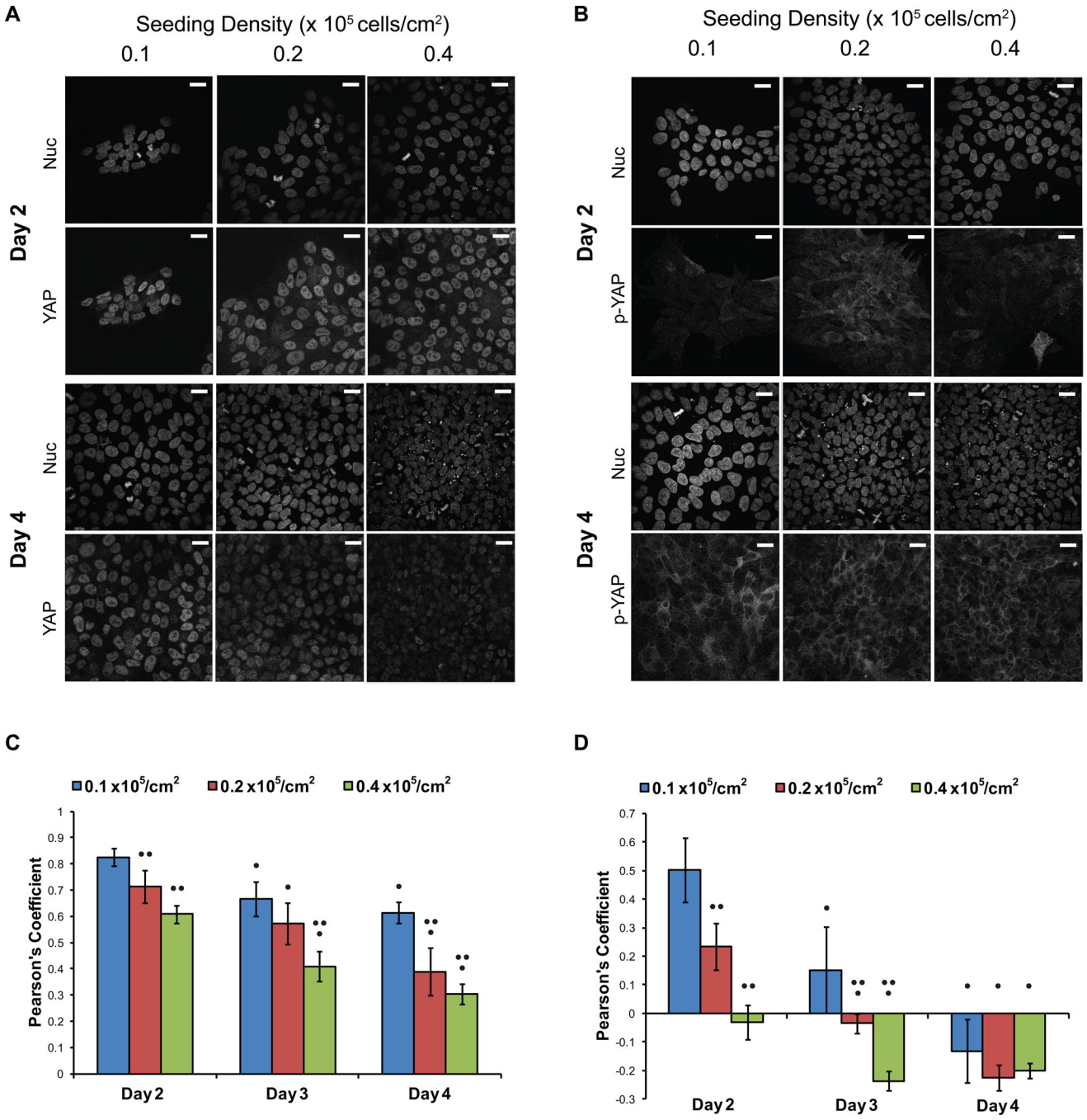

Figure 1.

YAP localization switched from nuclear to cytoplasmic as cell density increased. hPSCs were singularized and plated at 0.1, 0.2 and 0.4 × 10^5 cell/cm^2. Cells were fixed and stained after 2, 3 and 4 days of culture. (A, B) Representative confocal images of the nuclear Hoechst stain and (A) YAP immunofluorescence and (B) phospho-YAP (Ser127) immunofluorescence at days 2 and 4 are shown. Scale bars represent 10 μm. (C, D) Pearson's coefficients were calculated for 5 to 7 images and averaged for each condition to quantify the colocalization of YAP and phospho-YAP immunofluorescence with the Hoechst

stain. Pearson's coefficient of 1 represents complete colocalization, 0 represents no correlation and −1 represents negative correlation. (C) Colocalization of total YAP immunofluorescence and Hoechst. (D) Colocalization of phosphorylated YAP immunofluorescence and Hoechst. Error bars represent standard deviation. (• indicates $p<0.05$ compared to Day 2, •• indicates $p<0.05$ compared to 0.1×10^5 cell/cm^2 seeding density on the same day)

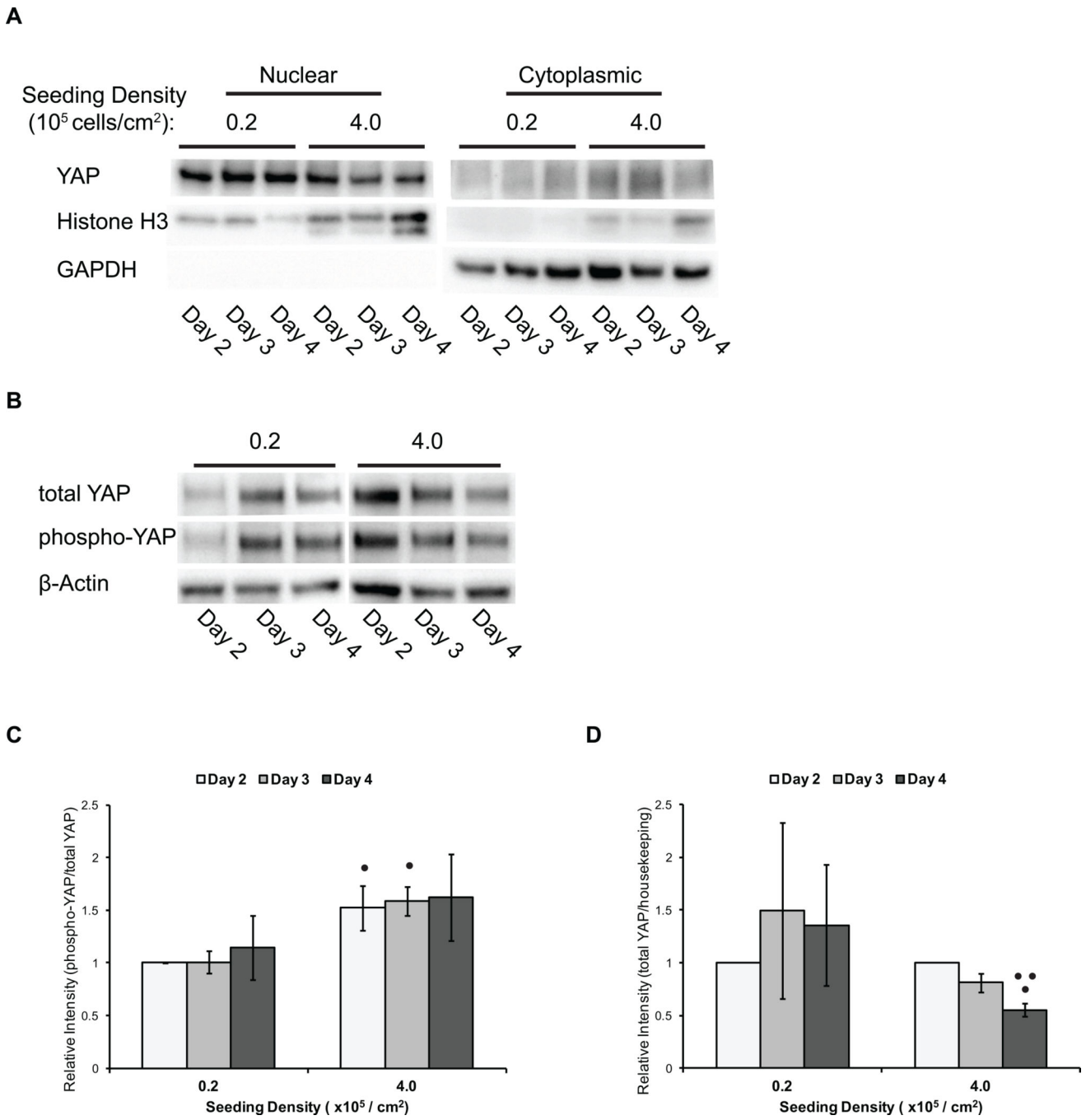

Figure 2.

YAP levels, localization and phosphorylation are modulated by hPSC density. hPSCs were singularized and plated at densities of 0.2 and 4.0 × 10^5 cell/cm^2. Cells were harvested for western blot analysis after 2, 3 and 4 days of culture. (A) Western blot analysis of total YAP, Histone H3 (nuclear control) and GAPDH (cytoplasmic control) in nuclear and cytoplasmic protein extracts. (B) Representative western blot analysis of total YAP, phospho-YAP (Ser127), and β-actin (housekeeping control) in whole cell lysates. (C) Semi-quantification of the ratio of phosphorylated YAP (Ser127) to total YAP protein by densitometry analysis

of western blots. Error bars represent standard deviation. (• indicates $p<0.05$ compared to 0.2×10^5 cell/cm^2 seeding density on the same day) (D) Semi-quantification of intensities of total YAP protein to β-actin by densitometry analysis of western blots. Error bars represent standard deviation. (• indicates $p<0.05$ compared to Day 2, •• indicates $p<0.05$ compared to Day 3)

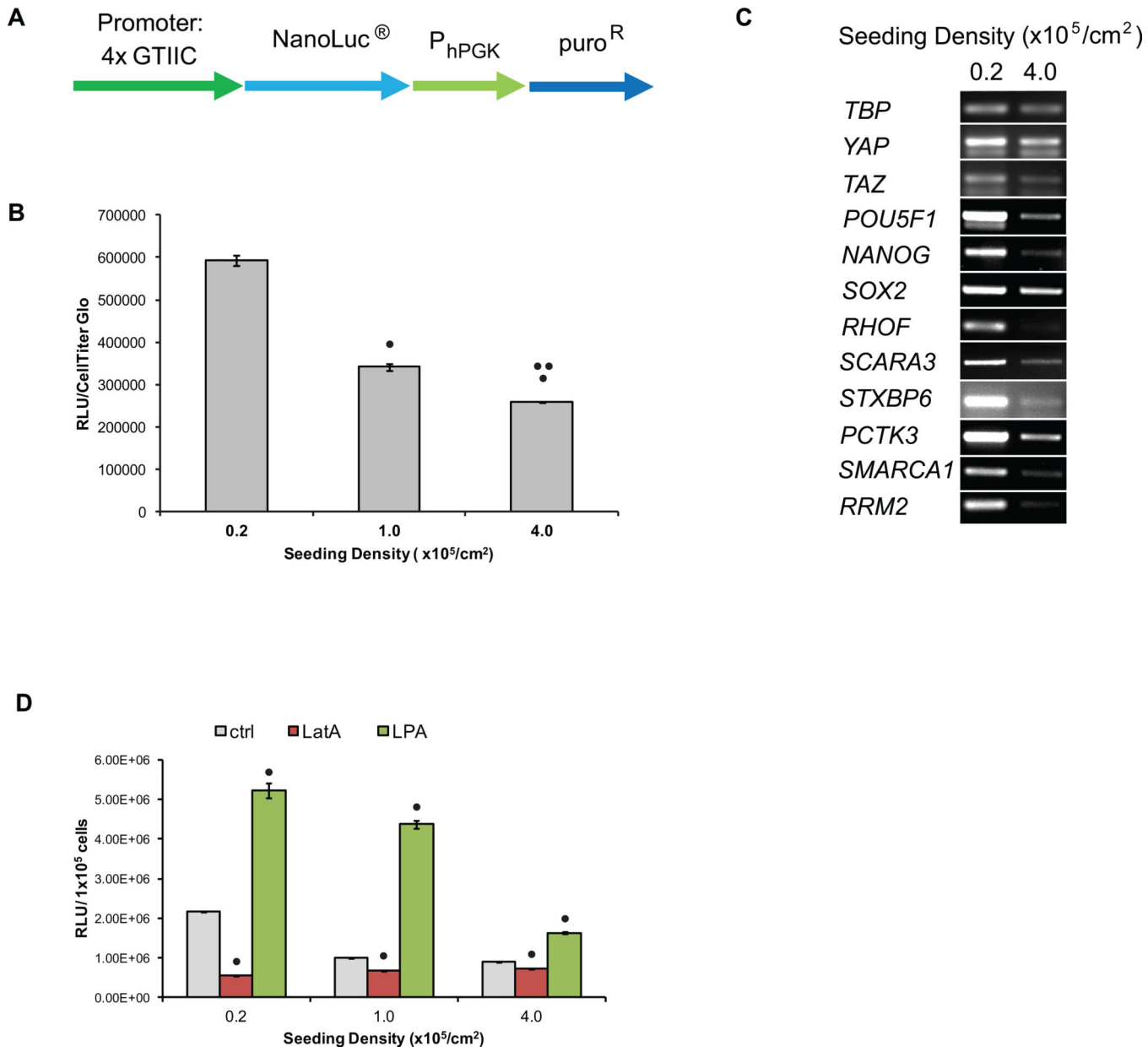

Figure 3.

YAP transcriptional activity decreased as hPSC density increased. (A) Schematic of YAP transcriptional reporter construct. 4xGTIIC are 4 repeats of TEAD binding sites (ACATTCCA) that drive expression of NanoLuc. (B) hPSCs were singularized and plated at densities of 0.2 to 4.0 × 10^5 cell/cm^2. After 3 days in culture, 100,000 cells were harvested for luciferase assays. Chemiluminescent signal was normalized to CellTiter-Glo signal. Error bars represent standard deviation. (• indicates $p<0.05$ compared to 0.2 ×10^5 cell/cm^2 seeding density, •• indicates $p<0.05$ compared to 1.0 ×10^5 cell/cm^2 seeding density) (C) After 3 days, RNA was extracted for end-point RT-PCR analysis of YAP target genes with TATA-box binding protein (*TBP*) expression serving as the housekeeping control. *YAP, TAZ, POU5F1* (Oct4), *NANOG* and *SOX2* expression were also analyzed. (D) H9

4xGTIIC-Nluc cells were singularized and plated at densities of 0.2 to 4.0 × 10^5 cell/cm^2. The following day, cells were treated with 1 μM LatA or 2 μM LPA. After 24 hours, cells were harvested for luciferase assays and the chemiluminescent signal was normalized to cell count. Error bars represent standard deviation. (• indicates $p<0.05$ compared to no treatment condition at the same seeding density)

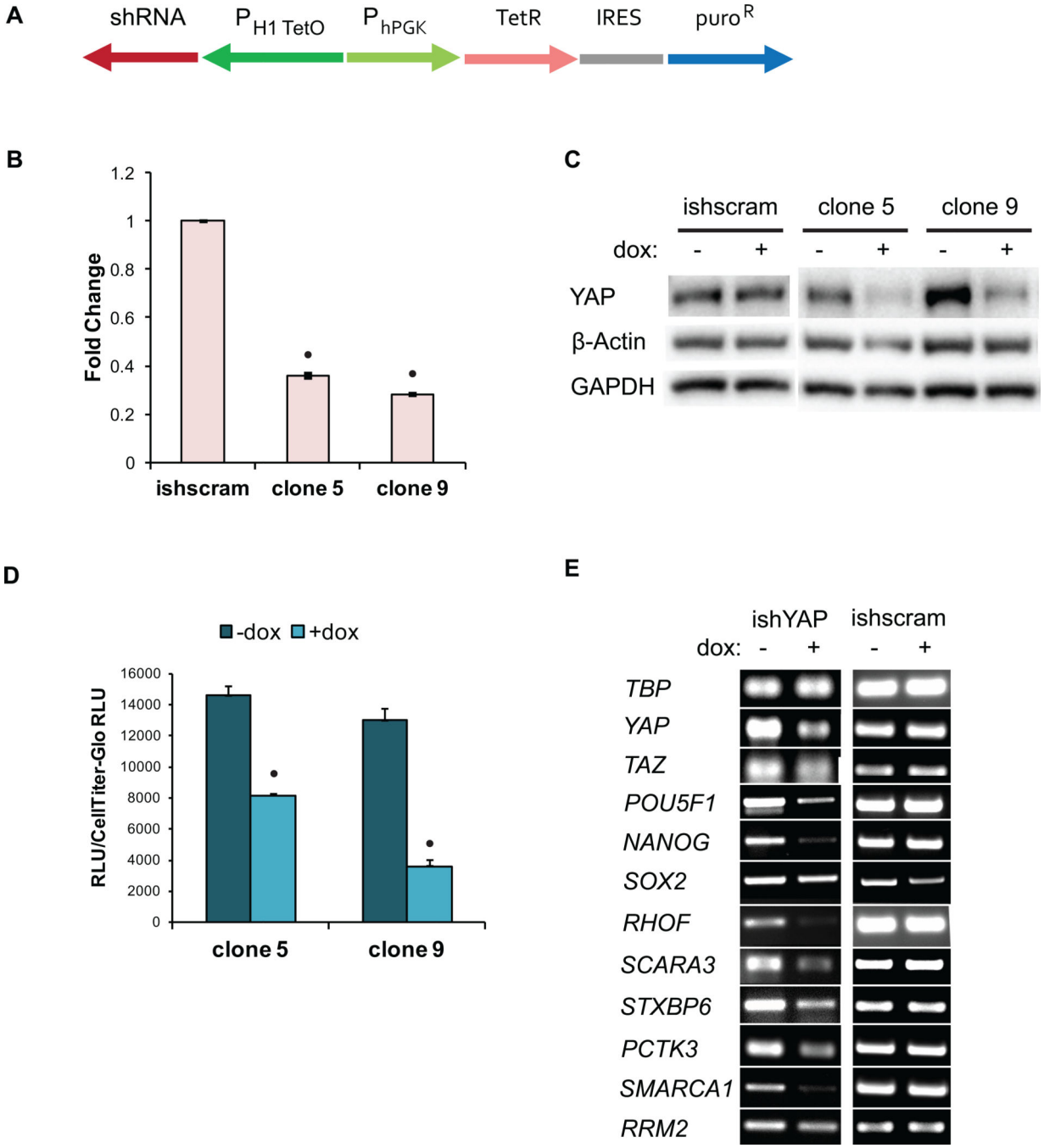

Figure 4.

YAP knockdown decreased YAP levels and transcriptional activity. (A) Schematic of construct for dox-inducible shRNA knockdown of YAP expression. PH1-TetO is the Tet-responsive human H1 promoter. H9 hESC YAP knockdown and scrambled sequence shRNA (ishscram) cell clones were plated at 0.2 $\times 10^5$ cell/cm^2 and treated with 2 μM doxycycline (dox) for 3 days and (B) harvested for qPCR analysis of YAP expression (• indicates $p<0.05$ compared to ishscram control) or (C) harvested for western blot analysis of YAP protein levels. (D) After 3 days of dox treatment, cells were transfected with the YAP responsive

8xGTIIC firefly luciferase plasmid. Following an additional 24 hours of dox treatment, cells were harvested for a luciferase assay. (• indicates $p<0.05$ compared to no dox condition) (E) Cells were treated with dox for 3 days and harvested for PCR analysis of YAP target genes, *YAP, TAZ, POU5F1* (Oct4), *NANOG* and *SOX2*.

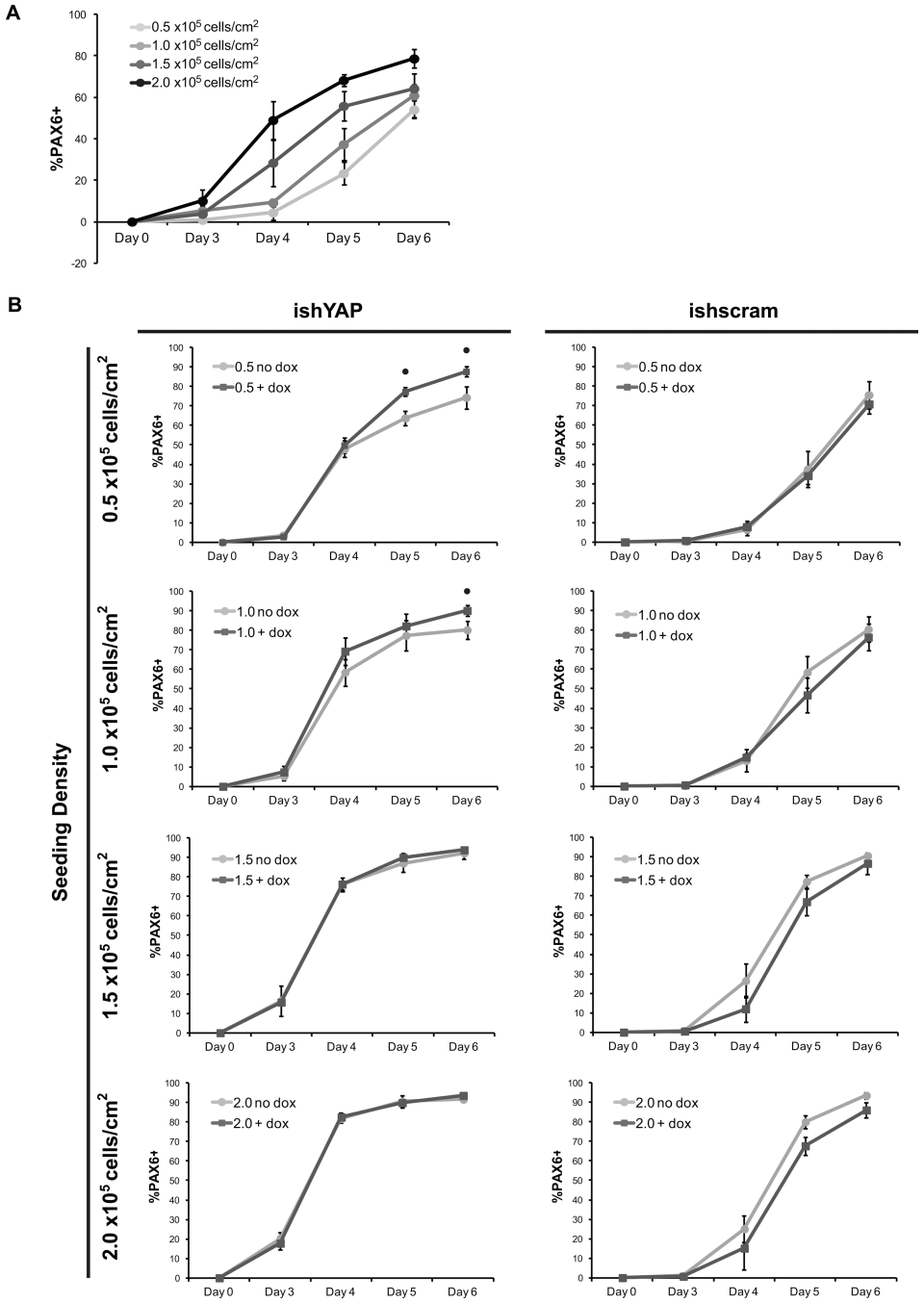

Figure 5.

High seeding density and YAP knockdown increased the conversion rate of hPSCs to PAX6+ neuroepithelial cells. (A) H9 hESCs were plated on Matrigel at densities of 0.5, 1.0, 1.5 and 4.0 × 10^5 cell/cm^2 in E8 medium and neuroepithelial differentiation was initiated the next day by changing the medium to E6. Flow cytometry for the percentage of PAX6-positive cells was performed through day 6 of differentiation. (B) Flow cytometry for percentage Pax6-positive cells was performed through day 6 utilizing H9 hESC inducible YAP knockdown (ishYAP) and inducible scrambled sequence shRNA (ishscram) cell lines.

Dox was added daily to fresh medium and compared to control cells with no dox added. Error bars represent standard deviation. (• indicates $p<0.05$ compared to no dox condition on the same-day)

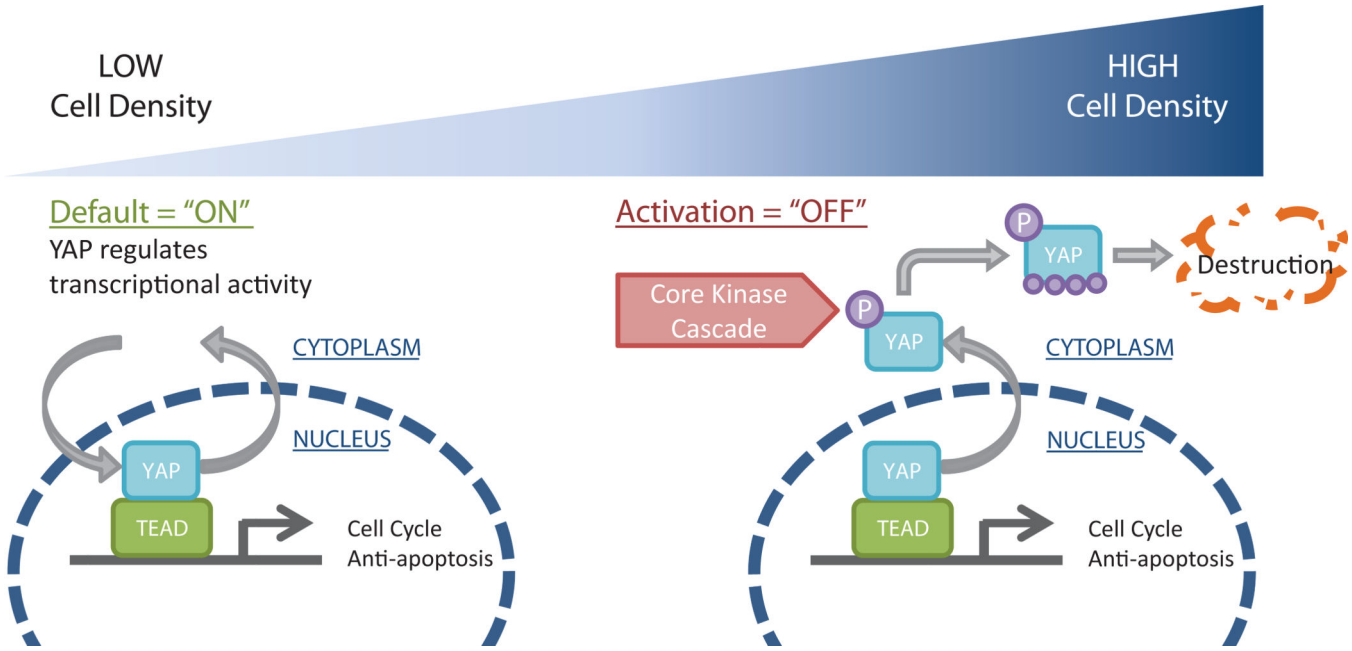

Figure 6.

Schematic model of the effects of hPSC density on YAP signaling. At low cell density (left), YAP is primarily localized to the nucleus where it associates with TEAD to regulate gene expression. At high cell density (right), YAP localizes to the cytoplasm where it is phosphorylated and destroyed.